

## Site-specific Effects of DUOX1-Related Peroxidase on Intercellular Apoptosis Signaling

SONJA HEINZELMANN\* and GEORG BAUER

*Institute of Virology, Department of Medical Microbiology and Hygiene,  
University of Freiburg, Freiburg, Germany*

**Abstract.** *Intercellular apoptosis-inducing HOCl signaling is known as an interplay between superoxide anions/H<sub>2</sub>O<sub>2</sub> of transformed target cells and dual oxidase 1 (DUOX1)-related peroxidase that is released from neighboring non-transformed or transformed effector cells. Effector cells are dispensable when the release of the peroxidase domain of DUOX1 from target cells is prevented through inhibition of matrix metalloproteinase (MMP) activity. Membrane-associated peroxidase is then co-localized to NADPH oxidase 1 (NOX1) and establishes HOCl signaling specifically in transformed cells, using the same biochemical pathways as classical intercellular HOCl signaling. Membrane-associated peroxidase protects against exogenous HOCl through reversal of the peroxidase reaction. In addition, membrane-associated peroxidase protects against NO/peroxynitrite signaling as it oxidates NO and decomposes peroxynitrite. The protective function of membrane-associated peroxidase (in the absence of MMP) is analogous to that of catalase, whereas the destructive effect of the enzyme, i.e. the synthesis of HOCl, is independent of its localization and of MMP activity.*

Intercellular apoptosis-inducing signaling through the HOCl signaling pathway and the NO/peroxynitrite signaling pathway is based on sustained NADPH oxidase 1 (NOX1)-dependent extracellular superoxide anion generation, which is specific for malignant cells (1-6). As intercellular apoptosis-inducing signaling causes selective elimination of malignant cells, it has been suggested to represent a potential

control step during oncogenesis (7-11). Intercellular HOCl signaling is based on extracellular superoxide anion generation by malignant cells (1-6), dismutation of superoxide anions to H<sub>2</sub>O<sub>2</sub>, utilization of H<sub>2</sub>O<sub>2</sub> by peroxidase (POD) for the synthesis of HOCl, and HOCl/superoxide anion interaction that leads to generation of apoptosis-inducing hydroxyl radicals. As further consequences, lipid peroxidation by hydroxyl radicals leads to the activation of sphingomyelinase, generation of ceramide and induction of the mitochondrial pathway of apoptosis, mediated by caspase-9 and caspase-3.

NO/peroxynitrite signaling depends on the formation of peroxynitrite through the interaction of malignant cell-derived superoxide anions with NO, resulting in the formation of peroxynitrite. Protonation of peroxynitrite leads to generation of peroxynitrous acid, which then decomposes into NO<sub>2</sub> and apoptosis-inducing hydroxyl radicals. Due to the action of proton pumps in the cell membrane, protonation of peroxynitrite seems to be favored over peroxynitrite/carbon dioxide interaction that might be inhibitory to NO/peroxynitrite signaling (12).

Whereas transformed cells are generally sensitive to apoptosis-inducing NO/peroxynitrite and HOCl signaling, tumor cells are protected against both pathways through expression of membrane-associated catalase (13, 14). Membrane-associated catalase decomposes H<sub>2</sub>O<sub>2</sub> and thus prevents HOCl synthesis. Catalytic decomposition of peroxynitrite and oxidation of NO by membrane-associated catalase efficiently interferes with NO/peroxynitrite signaling.

Our companion article in this issue dissected intercellular HOCl signaling into an interplay between NOX1-dependent target cell function, i.e. generation of extracellular superoxide anions, which is specific for malignant cells, and an effector function that is exerted by non-malignant and malignant cells with equal efficiency. The effector function was characterized as release of dual oxidase 1 (DUOX1)-related peroxidase. The experimental system was based on the analysis of dense clumps of target cells surrounded by effector cells in large number, but lower local density than

\*Present address: Eye Center, University Medical Center, Freiburg, Germany.

*Correspondence to:* Georg Bauer, Institut für Virologie, Department für Medizinische Mikrobiologie und Hygiene, Hermann-Herder Strasse 11, D-79104 Freiburg, Germany. E-mail: georg.bauer@uniklinik-freiburg.de

**Key Words:** NOX1, DUOX1, HOCl, apoptosis, matrix metalloproteinase.

the target cells. As shown in Figure 1, clumps of transformed target cells did not exhibit apoptosis induction when seeded alone. They were not able to establish significant HOCl signaling despite efficient generation of superoxide anions and H<sub>2</sub>O<sub>2</sub>, as their POD was released under the experimental conditions used and therefore was diluted below the effective concentration. When the clumps of transformed cells were surrounded by transformed or non-transformed effector cells, the supply of POD supported HOCl synthesis and apoptosis induction in the target cells (Figure 1 B). POD did not induce HOCl signaling in transformed effector cells, as their low cell density did not allow for sufficient generation of H<sub>2</sub>O<sub>2</sub> through dismutation of superoxide anions. Knockdown of *DUOX1* in the effector cells abrogated their effector function and thus allowed the conclusion that DUOX1 or a closely related protein was responsible for the effector function (Figure 1C). The addition of myeloperoxidase (MPO) allowed apoptosis induction in isolated clumps of transformed cells, indicating that POD activity is sufficient to explain the target cell function (Figure 1D). Directed measurement of POD release had shown that inhibition of matrix metalloproteinase (MMP) by galardin prevented the release of DUOX1-related POD. We speculated that galardin-pretreated isolated clumps of transformed target cells should be able to establish reactive oxygen species (ROS)-dependent apoptosis signaling, provided that the release of POD was not required as an activation step for the enzyme (Figure 1E).

## Materials and Methods

**Materials.** NOX1 inhibitor 4-(2-aminoethyl)benzenesulfonyl fluoride (AEBSF), catalase inhibitor 3-aminotriazole (3-AT), neutralizing monoclonal antibody directed against human catalase (anti-CAT), control antibody directed against laminin, catalase from bovine liver, NO donor diethylamine NONOate (DEA NONOate), NaOCl (for the generation of HOCl), the broad spectrum matrix metalloproteinase inhibitor (R)-N<sub>4</sub>-Hydroxy-N<sub>1</sub>-[(S)-2-(1*H*-indol-3-yl)-1-methylcarbonyl-ethyl]-2-isobutyl-succinamide (Galardin; GM6001) (15), hydroxyl radical scavenger mannitol, manganese-containing superoxide dismutase (MnSOD) from *Escherichia coli*, inhibitor of NO synthase (NOS) *N*-omega-nitro-L-arginine methylester hydrochloride (L-NAME), NOS inhibitor 3-bromo-7-nitroindazole (3-Br-7NI), HOCl scavenger taurine, H<sub>2</sub>O<sub>2</sub>-generating glucose oxidase (GOX) from *Aspergillus niger*, MPO from human leucocytes, xanthine and xanthine oxidase (XO) were obtained from Sigma Aldrich (Schnelldorf, Germany).

Transforming growth factor-β1 (TGFβ1) was purified from human platelets (16) and kept as a stock solution of 1.5 μg/ml in Eagle's minimal essential medium (EMEM) plus 5% fetal bovine serum (FBS) at -20°C.

Peroxynitrite and the peryoxynitrite decomposition catalyst 5-, 10-, 15-, 20-tetrakis(4-sulfonatophenyl)porphyrinato iron(III) chloride (FeTPPS) were obtained from Calbiochem/Merck Biosciences GmbH, Schwalbach/Ts, Germany. The mechanism-based peroxidase inhibitor 4-aminobenzoyl hydrazide (ABH) was obtained from Acros Organics, Geel, Belgium.

Inhibitors for caspase-3 (Z-DEVD-FMK) and caspase-9 (Z-LEHD-FMK) were obtained from R&D Systems (Wiesbaden-Nordenstadt, Germany).

The catalase mimetic EUK 134 [chloro{[2,2'-(1,2-ethanediylbis[(nitrilo-κN)methylidene]]bis[6-methoxyphenolato-κO]}manganese was a product of Cayman (Ann Arbor, MI, USA) and was obtained from Biomol (Hamburg, Germany).

**Media for cell culture.** Cells were either kept in EMEM, containing 5% FBS (Biochrom, Berlin, Germany) or in RPMI-1640 medium, containing 10% FBS, as indicated for the respective cell lines. FBS was heated for 30 minutes at 56°C prior to use. Both media were supplemented with penicillin (40 U/ml), streptomycin (50 μg/ml), neomycin (10 μg/ml), moronal (10 U/ml) and glutamine (280 μg/ml). All supplements were obtained from Biochrom. Cell culture was performed in plastic tissue culture flasks. Cells were passaged once or twice weekly.

**Cells.** Non-transformed rat fibroblasts 208F (17) and their derivative transformed through constitutive expression of v-src (208Fsrc3) (18), were a generous gift from Dr. C. Sers and Dr R. Schäfer, Berlin, Germany and were cultured in EMEM, with 5% FBS and supplemented as indicated above.

The gastric carcinoma cell line MKN-45 was purchased from the Deutsche Sammlung für Mikroorganismen und Zellkulturen, Braunschweig, Germany. Cells were grown in suspension, with some cells attaching to the plastic culture dish, in RPMI-1640, with 10% serum and supplements as described above. Care was taken to avoid cell densities below 300,000/ml and above 10<sup>6</sup>/ml.

The human Ewing sarcoma cell line SKN-MC was obtained from Dr. U. Kontny, Department of Pediatrics and Adolescent Medicine, University Medical Centre Freiburg, Germany and was cultured in EMEM with 5% fetal bovine serum and supplements as above.

**SiRNA-mediated knockdown of NOX1, DUOX1 and MMP2.** Control siRNA (siCo), siRNA against human NOX1 (siNOX1), against human DUOX1 (siDUOX1) and against human MMP2 (siMMP2) were obtained from Qiagen (Hilden, Germany) with the following sequences: siCo: sense: r(UUCUCCGAACGUGUCA CGU)dTdT, antisense: ACGUGACACGUUCGGAGAA)dTdT; siNOX1: sense: r(GACAAUACUACUACACAA)dTdT, antisense: r(UUGUGU AGUAGUAAUUGUC)dGdG; siDUOX1: sense: r(AGU CUA ACA CCA CAA CUA A)dTdT, antisense: r(UUA GUU GUG GUG UUA GAC U)dGdG. siMMP2 (H\_MMP2\_5\_HP Validated siRNA) was directed towards the target sequence: CAG GCT CTT CTC CTT TCA CAA. No information on the sequence of siMMP2 was available from the supplier.

siRNAs were dissolved in suspension buffer supplied by Qiagen at a concentration of 20 μM. Suspensions were heated at 90°C for 1 min, followed by incubation at 37°C for 60 minutes. Aliquots were stored at -20°C.

Before transfection, 88 μl of medium without serum and without antibiotics were mixed with 12 μl Hyperfect solution (Qiagen) and 1.2 μl specific siRNA or control siRNA. The mixture was treated by a Vortex mixer for a few seconds and then allowed to sit for 10 minutes. It was then gently and slowly added to 300,000 MKN-45 cells in 1 ml RPMI-1640 medium containing 10% FBS and antibiotics (12-well plates) or to 200,000 208F or 208Fsrc3 cells/well (6-well plates) plus 2.3 ml medium supplemented with 5% FBS and antibiotics. Thus the

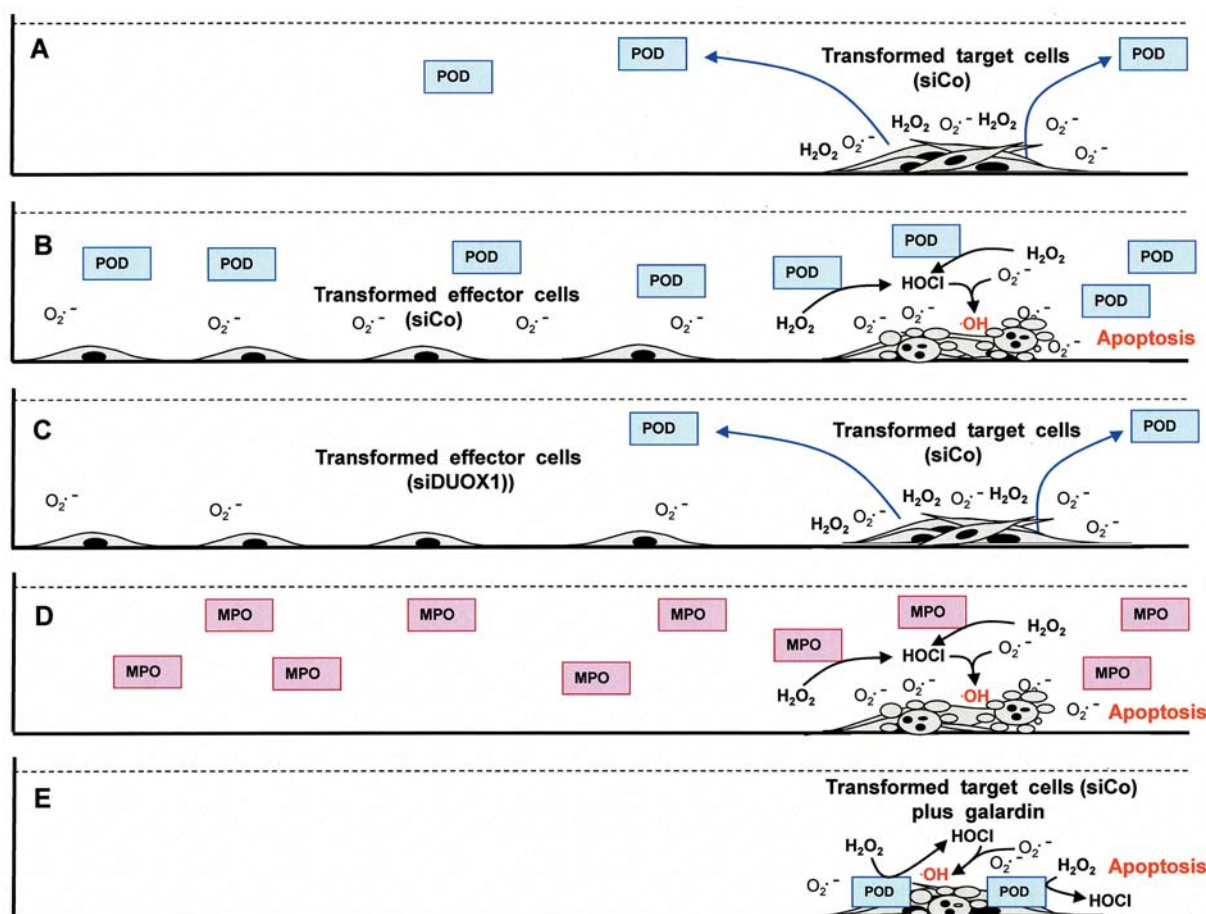


Figure 1. The concept of target and effector functions during intercellular HOCl signaling. The figure illustrates the experimental setup and the concepts established for intercellular apoptosis signaling through the HOCl signaling pathway. A: Despite high local concentrations of superoxide anions and  $H_2O_2$  in isolated dense clumps of transformed target cells, apoptosis does not take place as peroxidase (POD) is released from the cells and diluted in the surrounding medium. B: Neighboring transformed or (non-transformed) effector supply the target cells with POD and thus ensure selective apoptosis induction of the transformed target cells through HOCl signaling. Despite a sufficiently high concentration of released POD, transformed effector cells do not exhibit apoptosis induction as their low density does not support sufficient generation of  $H_2O_2$ . C: Knockdown of dual oxidase 1 (DUOX1) by small interfering RNA (siRNA) in the effector cells interferes with their effector cell function. D: The addition of soluble myeloperoxidase (MPO) is sufficient to support apoptosis-inducing HOCl signaling of the target cells. E: The working hypothesis here implies that prevention of the release of DUOX-coded POD through inhibition of matrix metalloproteinase using galardin should allow HOCl signaling in dense clumps of transformed target cells. The Figure summarizes the effects of transformed target cells 24 h after transfection with control siRNA (siCo) or with siRNA directed towards DUOX1 (siDUOX1). The effect of nontransformed effector cells is not shown, but is analogous to that of transformed effector cells.

concentration of siRNA was 24 nM for MKN-45 cells in suspension and 10 nM for 208F and 208Fsrc3 cells in monolayer. The cells were incubated at 37°C in 5%  $CO_2$  for 24 hours. Transfected cells were centrifuged and resuspended in fresh medium at the required density before use.

**Determination of the efficiency of siRNA-mediated knockdown.** The siRNA transfection system as described above had been optimized to allow a reproducible transfection efficiency of more than 95% of the cells and to avoid toxic effects (Bauer, unpublished result). We used a functional quantitation of knockdown efficiency, in line with the requirements of our experimental approach.

Functional knockdown of *NOX1* by siNOX1 was determined in 208Fsrc3 and MKN-45 cells through direct quantitation of superoxide anion production by siCo and siNOX1-transfected cells 24 h after transfection, following the protocol described by Temme and Bauer (19). Functional knockdown was at least 94%. The same result was obtained with a second siRNA directed towards *NOX1* (data not shown).

Functional knockdown of *DUOX1* by siDUOX1 was determined for 208Fsrc3 cells by direct quantitation of POD release from siCo and siDUOX1-transfected cells 24 h after transfection, using a recently described competition test for the quantitation of POD (20) which is described in our companion article. siDUOX1-mediated



functional knockdown of *DUOX1* was 88%. This result was confirmed through transfection with a second siRNA directed towards *DUOX1* (data not shown).

The efficiency of knockdown of *MMP2*-specific mRNA by siMMP2 was experimentally determined by the supplier, using real-time polymerase chain reaction and was found to be 92 % for 5 nM siRNA.

**Determination of the percentage of apoptotic cells.** The precise quantitative determination of the percentage of apoptotic cells in duplicate assays was the read-out for experiments that quantified i) apoptosis induction in isolated clumps of transformed target cells, ii) apoptosis induction in clumps of target cells surrounded by disperse effector cells, iii) autocrine apoptosis induction; iv) apoptosis induction by addition of exogenous HOC1, v) apoptosis induction by addition of the exogenous NO donor DEA NONOate and vi) apoptosis induction by addition of the exogenous peroxyntirite.

The percentage of apoptotic cells was determined by inverted phase-contrast microscopy based on the classical criteria for apoptosis, *i.e.* nuclear condensation or fragmentation and membrane blebbing (14, 21, 22). At least 2×200 cells were scored for each point of measurement in duplicate assays. Comparative analysis with several cell lines had shown that nuclear condensation/fragmentation as determined by inverse phase-contrast microscopy were correlated to intense staining with bisbenzimidazole, and to DNA strand breaks, detectable by the terminal deoxynucleotidyl transferase-mediated dUTP nick end labeling (TUNEL) reaction (8, 23-26). However, the TUNEL reaction was not used for routine quantitation, as the distinct steps during preparation of the samples caused a marked loss specifically of apoptotic cells.

**Apoptosis induction in isolated clumps of transformed target cells.** The experimental concept of this approach is explained in Figure 1. Transformed 208Fsrc3 cells, 24 h after transfection with 10 nM siCo, siNOX1 or siDUOX1 and nontransformed 208F cells 24 h after transfection with 10 nM siCo were seeded as clumps (2,000 cells in 5 µl medium, corresponding to 2,000 cells/mm<sup>2</sup>) in 12-well tissue culture clusters (two clumps per well). After the cells had attached to the well, 1 ml medium was added. Assays remained free of additions, or received 20 ng/ml TGFβ1, 200 mU/ml MPO, MPO plus TGFβ1 or MPO/TGFβ1/150 µM ABH. Alternatively, the clumps remained without further addition, or received 20 ng/ml TGFβ1, 10 µM galardin or galardin plus TGFβ1. The percentage of apoptotic cells was determined after 22 h in duplicate assays.

Transformed 208Fsrc3 cells, 24 h after transfection with 10 nM siCo, were seeded as clumps of 2000 cells/8 mm<sup>2</sup> in 12-well tissue culture clusters (2 clumps per well). After the cells had attached to the well, 1 ml complete medium was added. The assays remained without further addition, or received 20 ng/ml TGFβ1 or 10 µM galardin alone, or a combination of 10 µM galardin and 20 ng/ml TGFβ1. The following inhibitors were added singly: 100 U/ml MnSOD, 30 U/ml catalase, 150 µM ABH, 50 mM taurine, 10 mM mannitol, 2.4 mM L-NAME. The percentage of apoptotic cells was determined after 22 h in duplicate assays.

**Apoptosis induction in clumps of target cells surrounded by disperse effector cells.** This experimental approach allows to study the interaction between dispersely seeded effector cells and target cells seeded as clumps of high local density. Please see Figure 1 for

further explanation. Transformed 208Fsrc3 cells and nontransformed 208F cells were transfected with 10 nM siCo or siDUOX1. Twenty-four hours later, siCo- and siDUOX1-transfected 208Fsrc3 cells were seeded as clumps of 2,000 cells/8 mm<sup>2</sup> in 12 well tissue culture clusters. After the cells had attached to the well, 1 ml medium was added. Assays received either no effector cells or 12,000 208F effector cells transfected with either siCo or siDUOX1. TGFβ1 (20 ng/ml) was added to all assays. Where indicated, 10 µM galardin was added to the assays. After 22 h the percentage of apoptotic cells was determined in the clumps in duplicate experiments.

**Autocrine apoptosis induction.** When seeded at appropriate density as well as cell number, transformed cells or tumor cells (in the presence of an inhibitor or inactivator of their protective catalase) establish apoptosis-inducing intercellular ROS signaling. Assays of apoptosis were performed in 96-well plates with 100 µl of complete medium per well and contained either 12,500 transformed 208Fsrc3 cells plus 20 ng/ml TGFβ1, 12,500 MKN-45 cells plus anti-CAT (0, 8, 20, 51, 128, 320, 800 ng/ml) or 10,000 SKN-MC cells plus catalase inhibitor 3-AT (0, 25, 50, 100, 200 mM). The percentage of apoptotic cells was determined for MKN-45 cells after 4.5 h and for SKN-MC cells after 6.5 h.

208Fsrc3 cells received 0.4 mM xanthine in addition. Half of the cultures were treated with 10 µM galardin. XO was added at concentrations of 0, 0.15, 0.31, 0.62, 1.25 mU/ml. Control cultures received 0.6 µM of the catalase mimetic EUK-134. Some cultures received GOX (0, 1, 2 mU/ml), in the absence or presence of 0.6 µM EUK-134. The percentage of apoptotic cells was determined after 25 h.

In a further experiment, 208Fsrc3 cells received either no further addition (control) or 100 U/ml MnSOD, 150 µM ABH, 25 µM FeTPPS or 10 µM galardin. The cultures then received catalase from bovine liver (0, 2, 4, 8, 16, 31, 62, 125, 250, 500, 1000, 2000 U/ml) and were cultivated for 22 h before the percentages of apoptotic cells were determined.

Twenty-four hours after transfection of MKN-45 gastric carcinoma cells with 24 nM siCo, siDUOX1, siMMP2 or with siDUOX1 plus siMMP2, cells were seeded at a density of 12,500 cells/100 µl and received 150 mM ABH or 2.4 mM L-NAME. Anti-CAT was added at 0, 8, 20, 31, 128, 320, 800 ng/ml. The percentage of apoptotic cells was determined after 4 h. Parallel assays with antibody directed against laminin controlled the specificity of the effect of anti-CAT.

Twenty-four hours after transfection of SKN-MC cells 24 h after transfection with 10 nM of siCo, siDUOX1, siMMP2 or with siDUOX1 plus siMMP2, cells were seeded at a density of 10,000 cells per 100 µl assay and received either no further addition or 20 µM 3-Br-7NI, 100 µM AEBBSF, 25 µM FETPPS, 20 mM mannitol, 25 µM caspase-9 inhibitor, 50 µM caspase-3 inhibitor, 150 µM ABH or 10 µM galardin. 3-AT was added (0, 25, 50, 100, 200 mM) and the percentages of apoptotic cells were determined after 6.5 h.

**Apoptosis induction by addition of exogenous HOC1.** Twenty-four hours after transfection with 24 nM siCo or siDUOX1, MKN-45 tumor cells were seeded at a density of 12,500 cells per 100 µl in 96-well tissue culture clusters. Where indicated, 10 µM galardin and/or 150 µM ABH were added. After 30 minutes, HOC1 was added at the indicated concentrations. The percentage of apoptotic cells was determined after 1 h.

*Apoptosis induction by addition of the exogenous NO donor DEA NONOate.* A total of 12,500 208Fsrc3 cells/100  $\mu$ l complete medium plus 20 ng/ml TGF $\beta$ 1 were treated with 150  $\mu$ M ABH, 10  $\mu$ M galardin, 150  $\mu$ M ABH plus 10  $\mu$ M galardin, 40  $\mu$ M FeTPPS or 150 U/ml MnSOD. After 30 min, the NO donor DEA NONOate was added at 0, 15, 31, 62, 125, 250, 500, 1000  $\mu$ M. The percentages of apoptotic cells were determined after 3 h at 37°C.

*Apoptosis induction by addition of exogenous peroxynitrite.* A total of 10,000 208Fsrc3 cells/100  $\mu$ l complete medium remained untreated or were treated with 10  $\mu$ M galardin or 10  $\mu$ M galardin plus 150  $\mu$ M ABH. After 30 min, peroxynitrite (0, 25, 50, 100  $\mu$ M) was added and the percentages of apoptotic cells were determined after 4.5 h. In another experiment, 10 000 208Fsrc3 cells/100  $\mu$ l remained untreated or were treated with 150  $\mu$ M ABH, 200 mU/ml MPO, or 200 mU/ml MPO plus 150  $\mu$ M ABH. The assays received peroxynitrite (0, 25, 50, 100  $\mu$ M) and the percentages of apoptotic cells were determined after 5 h.

*Statistics.* In all experiments, assays were performed in duplicate. The mean values and the empirical standard deviation were calculated from parallel assays and are shown in the figures. Absence of standard deviation bars for certain points indicates that the standard deviation was too small to be reported by the graphic program, *i.e.* that results obtained in parallel were nearly identical. Empirical standard deviations were calculated merely to demonstrate how close the results were obtained in parallel assays within the same experiment and not with the intention of statistical analysis of variance, which would require larger numbers of parallel assays. Standard deviations were not calculated between different experiments, due to the usual variation in kinetics of complex biological systems *in vitro*.

The key experiments were performed five times, all other experiments at least twice.

The Yates continuity corrected chi-square test was used for the statistical determination of significance differences between data.

## Results

*Supply with optimal POD concentration is required for apoptosis induction in isolated clumps of transformed target cells.* Our companion article in this issue showed that apoptosis induction through the HOCl signaling pathway in isolated clumps of transformed cells requires the presence of surrounding nontransformed or transformed effector cells. These contributed to the establishment of intercellular apoptosis inducing ROS signaling through supply with DUOX1-coded POD activity. Alternatively, soluble MPO at sufficiently high concentration substituted for the effector function. Therefore, for a more detailed analysis, MPO was added to transformed target cells or nontransformed 208F cells seeded in clumps. The transformed target cells had been transfected with siCo or siNOX1 or siDUOX1. In the presence of MPO, transformed cells with functional NOX1 (*i.e.* 208Fsrc3 siCo and 208Fsrc3 siDUOX1), but not 208Fsrc siNOX1 or non-transformed 208F cells, responded with apoptosis induction ( $p < 0.001$ ) (Figure 2A). As apoptosis induction was inhibited by ABH ( $p < 0.001$ ), the

functional role of MPO enzymatic activity for this NOX1-dependent process was proven. Interestingly, apoptosis induction in the presence of MPO was enhanced by TGF $\beta$ 1 ( $p < 0.001$ ). As TGF $\beta$ 1 was recently shown by us to trigger NOX1 activity (19), this finding points to a requirement for enhancement of superoxide anion generation for optimal HOCl synthesis mediated by MPO.

In order to test for the functionality of membrane-associated DUOX1-related POD, we treated clumps of transformed target cells (208Fsrc3siCo, 208Fsrc3 siNOX1, 208Fsrc3siDUOX1) as well as of non-transformed 208F cells with the MMP inhibitor galardin, both in the absence and presence of TGF $\beta$ 1, and tested for apoptosis induction. Clumps without further addition or with sole TGF $\beta$ 1 or galardin treatment only showed marginal induction of apoptosis (Figure 2B). In contrast, treatment with TGF $\beta$ 1 plus galardin caused strong apoptosis induction in 208Fsrc siCo cells ( $p < 0.001$ ), but not in 208Fsrc3 siNOX1, 208Fsrc3 siDUOX1 or in non-transformed 208F cells. This finding demonstrates that localization of DUOX1 peroxidase close to NOX1 renders transformed target cells independent of the action of surrounding effector cells and allows apoptosis induction. This finding confirms the interaction between DUOX1 and NOX1, provided the cells were stimulated by TGF $\beta$ 1. Although non-transformed 208F cells have the potential to express the POD domain of DUOX1 (as shown in our companion article), their lack of NOX1 expression seems to render them insensitive to apoptosis induction even if DUOX-related POD remains associated with the cell membrane in the presence of galardin.

Apoptosis induction in transformed cell clumps in the presence of galardin and TGF $\beta$ 1 ( $p < 0.001$ ) was dependent on superoxide anions, H<sub>2</sub>O<sub>2</sub>, POD activity, HOCl and hydroxyl radicals, as apoptosis was blocked by the superoxide anion scavenger SOD, H<sub>2</sub>O<sub>2</sub>-decomposing catalase, peroxidase inhibitor ABH, HOCl scavenger taurine and the hydroxyl radical scavenger mannitol ( $p < 0.001$ ) (Figure 3). These essential elements establish the classical HOCl signaling pathway (7, 9). Apoptosis induction in the presence of galardin was only marginally inhibited by the NOS inhibitor L-NAME, indicating that NO/peroxynitrite signaling played no essential role under these conditions.

*Formal proof for the action in trans of the POD domain of DUOX1 released from effector cells.* Although the characteristics of the target/effector cell system as studied in our preceding article indicated that the POD domain of DUOX1 was released and acted in trans on malignant target cells, no formal proof for the important aspect of the site of action had yet been provided. The finding that the release of the DUOX1-related POD was inhibited by galardin allowed us to address this question. Therefore, clumps of transformed 208Fsrc3siCo and 208Fsrc3siDUOX1 cells were cultured

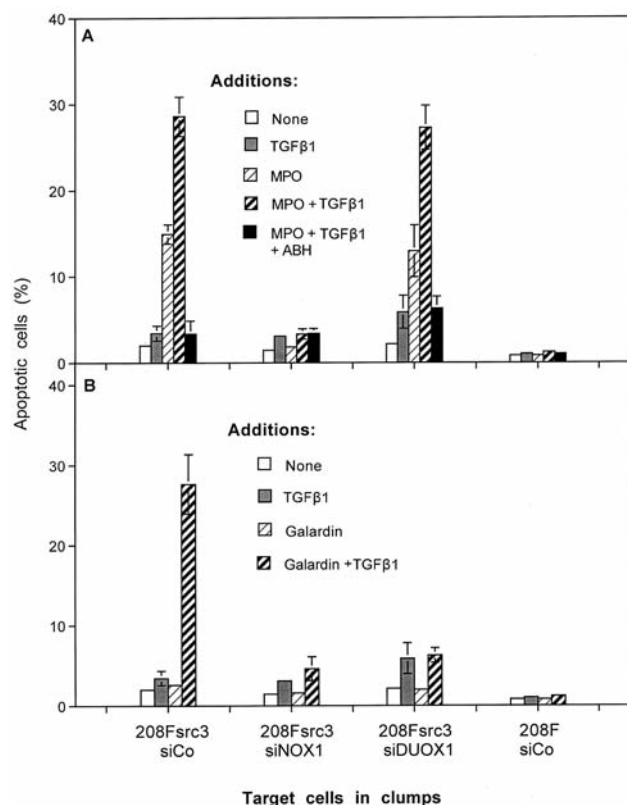


Figure 2. A: Myeloperoxidase (MPO) is sufficient to mediate apoptosis induction in clumps of NADPH oxidase1 (NOX1)-expressing transformed cells. In the presence of transforming growth factor-β1 (TGFβ1), MPO causes apoptosis induction in transformed 208Fsrc3 cells transfected with control small-interfering RNA (siRNA) (siCo) or siRNA directed towards dual oxidase1 (siDUOX1), but not in transformed cells transfected with siRNA directed towards NADPH oxidase 1 (siNOX1) or in siCo-transfected non-transformed 208F cells. The effect of MPO is abrogated by the peroxidase inhibitor aminobenzoyl hydrazide (ABH). B: Inhibition of matrix metalloproteinase (MMP) by galardin establishes apoptotic signaling in isolated clumps of transformed cells: requirement for NOX1 and DUOX1 at the same site. Treatment with the MMP inhibitor galardin plus TGFβ1 allows for apoptosis induction in transformed 208Fsrc3siCo cells, but not in 208Fsrc3siNOX1, 208Fsrc3siDUOX1 or non-transformed 208FsiCo cells. Data are mean values ± standard deviation. The presented experiment is representative of five independent experiments.

without effector cells or in the presence of 208F effector cells. The effector cells had been transfected either with control siRNA (siCo) or siRNA directed against DUOX1 (siDUOX1). The assays were cultivated in the absence or presence of the MMP inhibitor galardin. As shown in Figure 4, in the absence of galardin, 208Fsrc3siCo as well as 208Fsrc3siDUOX1 target cells responded with apoptosis induction in the presence of 208FsiCo, but not 208FsiDUOX1 effector cells, confirming that DUOX1 is associated with the effector cell function but not with the

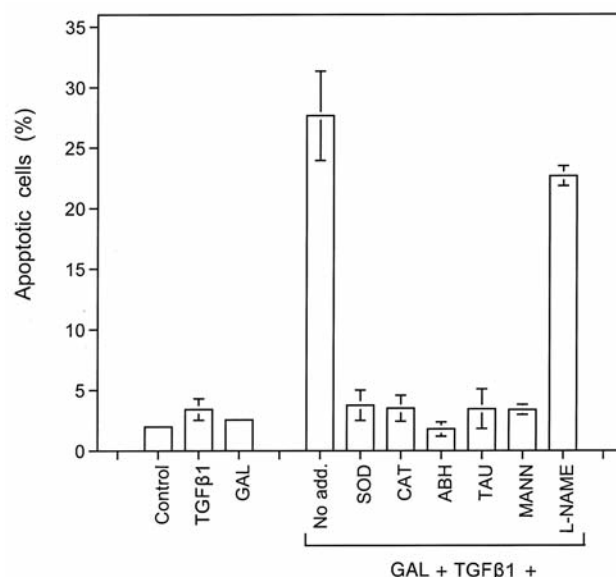


Figure 3. HOCl signaling in isolated clumps of 208Fsrc3 cells after galardin treatment. Apoptosis induction in clumps of transformed 208Fsrc3 cells mediated by galardin (GAL) plus transforming growth factor-β1 (TGFβ1) is inhibited when superoxide anions are scavenged by superoxide dismutase (SOD), hydrogen peroxide is decomposed by catalase (CAT), peroxidase is inhibited by 4-aminobenzoyl hydrazide (ABH), HOCl is scavenged by taurine (TAU) and hydroxyl radicals are scavenged by mannitol (MANN), whereas inhibition of NO synthase (NOS) by N-omega-nitro-L-arginine methylester hydrochloride (L-NAME) has no effect. Data are mean values ± standard deviation. The presented experiment is representative of three independent experiments.

target cell function. In the presence of galardin, 208Fsrc3siCo target cells showed apoptosis induction independent of the presence of effector cells ( $p < 0.001$ ), as galardin prevented the release of POD from the target cells and thus enabled their own apoptotic signaling. When, however clumps of 208Fsrc3siDUOX1 target cells were cultivated in the presence of galardin, there was no significant apoptosis induction due to the lack of POD. In the presence of galardin, apoptosis induction in siDUOX1 target cells was not resumed by surrounding 208FsiCo effector cells. This finding indicates that DUOX1 has to be released by the effector cells and has to interact in *trans* with the clump of target cells.

*Site-specific effects of membrane-associated DUOX1 on the HOCl signaling pathway.* The experimental option to restrict the localization of DUOX1-related POD to the membrane of transformed cells through inhibition of MMP allowed us to study site-specific effects of ROS interaction in HOCl signaling. When HOCl signaling was allowed in 208Fsrc3 cells, the addition of soluble superoxide anion-generating

XO caused a concentration-dependent inhibition of apoptosis induction ( $p < 0.001$ ) (Figure 5A). Based on our concept of HOCl signaling (7, 9, 27) this decrease was explained as HOCl/superoxide anion interaction leading to the formation of hydroxyl radicals distant from the cell membrane. These were ineffective in apoptosis induction as they could not reach the cell membrane due to their small free-diffusion path length. This concept was proven to be correct, as inhibition of POD release by galardin completely prevented XO-dependent inhibition of HOCl signaling ( $p < 0.001$ ) (Figure 5A). This result is in line with the assumption that in the presence of galardin, POD localized in close vicinity to the cell membrane restricted HOCl synthesis to this site and thus favored HOCl/superoxide anion interaction and hydroxyl radical formation in close vicinity of the membrane. As the catalase mimetic EUK-134 did not interfere with XO-mediated inhibition of HOCl signaling in the absence of galardin (Figure 5B), an alternative explanation through interference of  $H_2O_2$  with HOCl signaling was excluded, especially as the concentration of EUK-134 chosen was shown to interfere with the inhibitory effect of  $H_2O_2$ -generating GOX ( $p < 0.01$ ) (Figure 5C).

*DUOX1-mediated protection against exogenous HOCl.* MKN-45 human gastric carcinoma cells interfere with autocrine apoptosis-inducing HOCl signaling through their membrane-associated catalase (14) that decomposes  $H_2O_2$  and thus prevents HOCl synthesis. However, exogenous HOCl induces apoptosis in MKN-45 cells, as their generation of extracellular superoxide anions is sufficient to drive HOCl/superoxide anion interaction ( $HOCl + O_2^{\bullet-} \rightarrow \bullet OH + Cl^- + O_2$ ) (28). This was experimentally confirmed in the experiment shown in Figure 6A, where apoptosis was induced in siCo-transfected MKN-45 cells, dependent on the concentration of exogenous HOCl ( $p < 0.001$ ). Pre-treatment of the cells with galardin strongly interfered with subsequent apoptosis induction by exogenous HOCl ( $p < 0.001$ ). This protective effect was completely abrogated in the presence of the peroxidase inhibitor ABH ( $p < 0.001$ ), indicating that it was due to the catalytic activity of POD. DUOX1 was defined as the responsible enzyme, as siDUOX1-transfected MKN-45 cells were not protected against exogenous HOCl ( $p < 0.001$ ) despite the presence of galardin (Figure 6B). The requirement for inhibition of MMP indicates that a site-specific localization of DUOX1 POD on the membrane allowed for protection against the apoptosis-inducing effect of exogenous HOCl.

*DUOX1-mediated protection against exogenous NO/peroxynitrite signaling.* Addition of the NO donor DEA NONOate to 208Fsrc3 cells caused rather rapid apoptosis induction in a concentration-dependent mode ( $p < 0.001$ )

(Figure 7). Apoptosis induction required the presence of the NO donor and was inhibited by SOD and by the peroxynitrite decomposition catalyst FeTPPS ( $p < 0.001$ ), indicating that peroxynitrite formation through the reaction of superoxide anions with NO represented the central step in apoptosis signaling. As expected from previous studies, POD was not required for NO/peroxynitrite signaling, as ABH did not show any inhibitory effect. However, in the presence of galardin, *i.e.* conditions where DUOX1 release was prevented, NO-dependent, peroxynitrite-mediated apoptosis induction mediated by DEA NONOate in the concentration range between 15 and 125  $\mu M$  was completely blocked ( $p < 0.001$ ) and was partially blocked at concentrations of DEA NONOate higher than 125  $\mu M$  ( $p < 0.01$ ). This inhibitory effect was abrogated by ABH ( $p < 0.001$ ), indicating that a catalytic action of POD was responsible for inhibition of NO/peroxynitrite signaling.

For a direct test of potential peroxynitrite decomposition, 208Fsrc3 cells that had been treated with galardin were challenged by addition of peroxynitrite. In the absence of galardin, the cells exhibited apoptosis induction dependent on the concentration of peroxynitrite added ( $p < 0.001$ ) (Figure 8A). In the presence of galardin, the cells were protected against apoptosis induction by peroxynitrite through the action of POD, as protection was abrogated in the presence of ABH ( $p < 0.001$ ). An analogous, although less pronounced protective effect was seen when soluble MPO was added to the cells before peroxynitrite treatment ( $p < 0.001$ ) (Figure 8B). The partial protection by MPO was abrogated by ABH ( $p < 0.001$ ), pointing to the specific role of the peroxidase function for the protective effect.

Transformed 208Fsrc3 cells at standard density (125,000 cells/ml) and in the presence of TGF $\beta$ 1 led to autocrine apoptosis induction ( $p < 0.001$ ) that was dependent on superoxide anions (inhibition by SOD) ( $p < 0.001$ ), POD (inhibition by ABH) ( $p < 0.001$ ), but not on NO/peroxynitrite signaling (no inhibition by FeTPPS). (Figure 9A). Addition of gradually increasing concentrations of catalase inhibited HOCl signaling ( $p < 0.001$ ) and, after complete inhibition allowed resumption of apoptosis induction that was completely dependent on NO/peroxynitrite signaling ( $p < 0.001$ ). At very high concentrations of catalase, NO/peroxynitrite signaling was also inhibited ( $p < 0.001$ ). The resumption of NO/peroxynitrite signaling through catalase was due to abrogation of a  $H_2O_2$ -mediated consumption reaction directed against NO. Catalase in the concentration range around 250 U/ml allowed optimal enhancement of NO/peroxynitrite signaling, whereas much higher concentrations of catalase were required for the inhibition of NO/peroxynitrite signaling through peroxynitrite decomposition. In line with our previous findings, HOCl signaling was not affected when galardin had prevented the



release of the POD domain, whereas NO/peroxynitrite signaling at catalase concentrations higher than 16 U/ml was effectively inhibited ( $p<0.001$ ) (Figure 9B).

The data obtained so far show that localization of the POD domain of DUOX1 to the cell membrane through inhibition of matrix metalloproteinases caused an inhibitory effect on NO/peroxynitrite signaling that was analogous to the protective effect of membrane-associated catalase, but that there was no negative influence on HOCl signaling by membrane-associated DUOX1-related POD, in contrast to catalase which interferes with HOCl signaling. For an analysis of this selectivity and partial analogy between membrane-associated DUOX1-related POD and catalase, MKN-45 gastric carcinoma cells were treated with increasing concentrations of neutralizing antibody directed towards human catalase (Figure 10). In line with previous findings, inhibition of membrane-associated catalase caused apoptosis induction in the mode of an optimum curve ( $p<0.001$ ) that was dependent on NO/peroxynitrite signaling at low concentration of antibody, followed by HOCl signaling at higher ones ( $p<0.001$ ) (Figure 10 A). In the presence of galardin, NO/peroxynitrite signaling was completely inhibited ( $p<0.001$ ), whereas HOCl signaling was not affected (Figure 10 B). Inhibition of NO/peroxynitrite signaling was due to the enzymatic function of POD as it was abrogated by the peroxidase inhibitor ABH ( $p<0.001$ ). Knockdown of *DUOX1* activity inhibited HOCl signaling ( $p<0.001$ ), but had no effect on NO/peroxynitrite signaling, independent of the absence or presence of galardin. This finding indicates that *DUOX1*-encoded peroxidase is responsible for inhibition of NO/peroxynitrite signaling in the presence of galardin. The effect of the MMP inhibitor was mimicked by knockdown of *MMP2* ( $p<0.001$ ), in line with the established concept of the localization of the POD domain at the membrane when MMPs were inhibited or absent (Figure 10E and F).

Tumor cell lines derived from mammary carcinoma, small cell lung carcinoma, ovarian carcinoma, neuroblastoma and Ewing sarcoma have been found to re-activate NO/peroxynitrite signaling exclusively after inhibition of their protective catalase (14; Bauer, unpublished results). Figure 11A shows that the catalase inhibitor 3-AT caused concentration-dependent apoptosis induction in the Ewing sarcoma cell line SKN-MC in the mode of a plateau curve ( $p<0.001$ ). Apoptosis induction was dependent on superoxide anions, NO and peroxynitrite, as deduced from the inhibitor profile ( $p<0.001$ ). Apoptosis induction was mediated by caspase 3 and caspase 9 ( $p<0.001$ ) (Figure 11B). Inhibition of MMP (Figure 11C) and knockdown of *MMP2* (Figure 11D) caused a strong inhibition of apoptosis induction through the action of DUOX1-related POD ( $p<0.001$ ), as it was abrogated by ABH and by knockdown of *DUOX1* ( $p<0.001$ ).

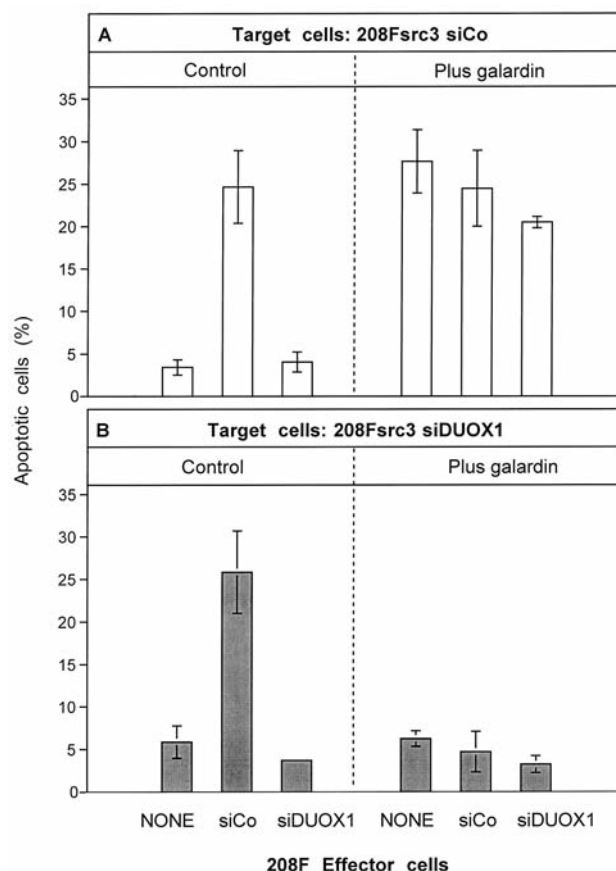


Figure 4. Dual oxidase 1 (DUOX1)-related peroxidase needs to be released from the effector cells and to act at the site of target cells. The effector function of 208F cells surrounding a clump of transformed 208Fsrc3 cells is abrogated through siRNA-mediated knockdown of DUOX1 in the effector cells, but not in the target cells. Data are mean values  $\pm$  standard deviation. The presented experiment is representative of two independent experiments.

## Discussion

Our companion article has shown that the HOCl signaling pathway requires i) NOX1-expressing malignant target cells at sufficiently high cell density and ii) a sufficient number of DUOX1-expressing nontransformed or transformed effector cells. The establishment of HOCl synthesis is satisfactorily explained by the activity of POD, as seen by the inhibitory effect of the POD inhibitor ABH and as purified soluble MPO mimics the effector cell function. Here we show explicitly that establishment of HOCl signaling requires either that DUOX1-coded POD is released from surrounding effector cells and acts at the site of transformed target cells, or that POD release from transformed target cells is prevented through inhibition of MMP, thus co-localizing



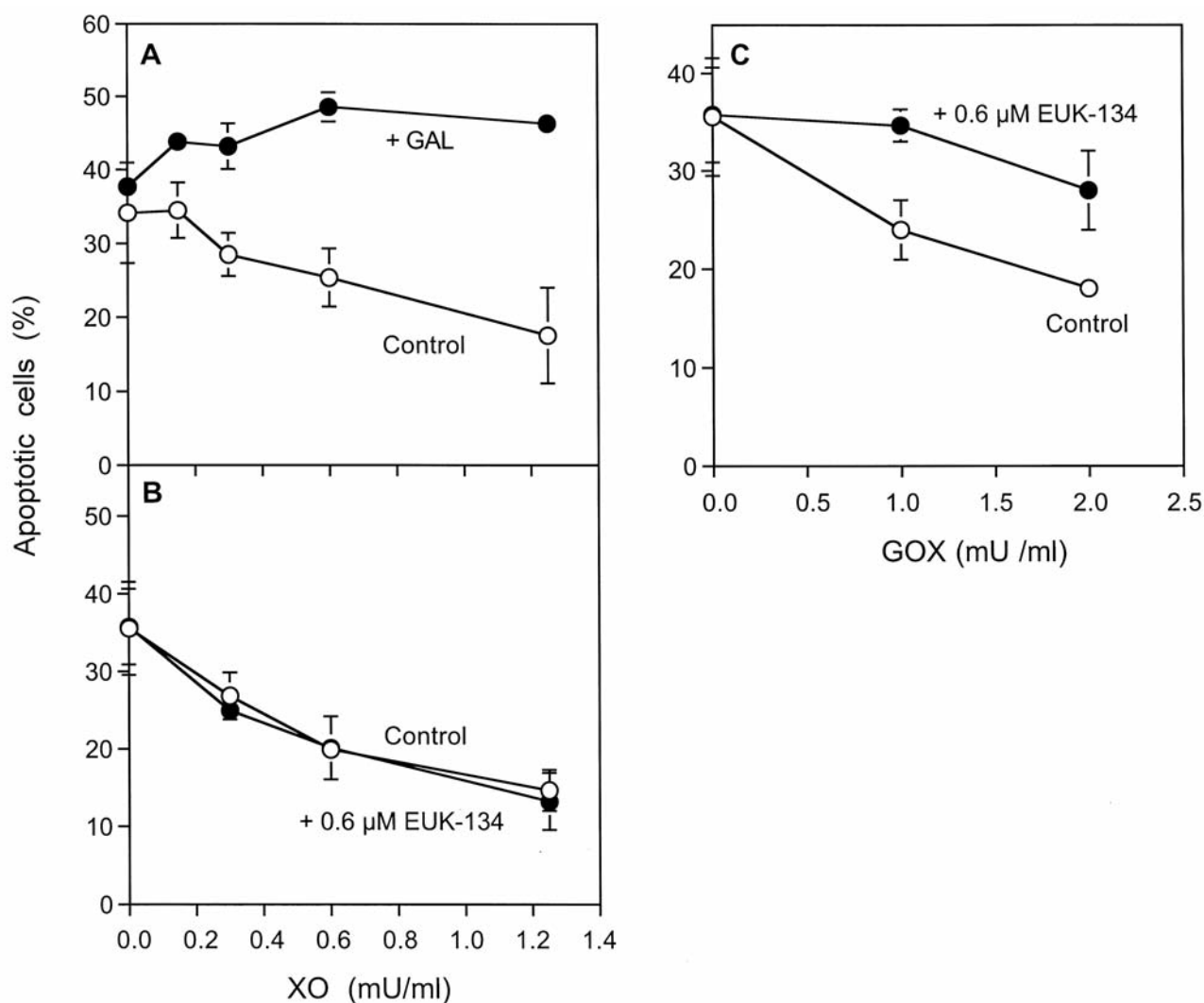


Figure 5. The importance of site-specific HOCl/superoxide anion interaction. Autocrine apoptosis induction in 208Fsrc3 cells is inhibited through random generation of superoxide anions by xanthine oxidase (XO) plus xanthine. This inhibitory effect is prevented when peroxidase release is prevented by galardin (GAL) and thus HOCl synthesis occurs close to the membrane of the transformed cells (A). The inhibitory effect of XO is not due to excess production of hydrogen peroxide (B), as it is not inhibited by the catalase mimetic [chloro([2,2'-(1,2-ethanediyl)bis[(nitrilo-κN)methylidyne]]bis[6-methoxyphenolato-κO]-manganese (EUK-134). Thus, it is different from the H<sub>2</sub>O<sub>2</sub>-dependent effect mediated by glucose oxidase (GOX) (C). Data are mean values ± standard deviation. The presented experiment is representative of five independent experiments.

NOX1 and DUOX1 in the direct vicinity on the membrane of the transformed target cells. Prevention of the release of the POD domain from NOX1-expressing target cells at high local density, thus substitutes for surrounding effector cells, as it localizes superoxide anion synthesis, dismutation of superoxide anion and HOCl synthesis at the same site, *i.e.* the membrane of transformed target cells. The resultant signaling pathway is analogous to that seen in the interaction between target and effector cells, as shown by the inhibition profile. Non-transformed cells that express DUOX1, but lack active NOX1, do not support autocrine HOCl signaling. This

indicates that the residual NOX domain of DUOX1 does not significantly contribute to superoxide anion generation. The interplay between NOX1 and membrane-associated DUOX1 in malignant cells requires the activity of TGFβ1, which seems to enhance the expression or activity of both partners.

As DUOX1-coded POD localized to the membrane after inhibition of MMP is as efficient as free POD at sufficiently high concentration, it is obvious that the release of the POD domain through MMP is not linked to a hypothetical activation step. However, the localization of the POD to the membrane has site-specific effects on HOCl signaling, as the synthesis of HOCl is

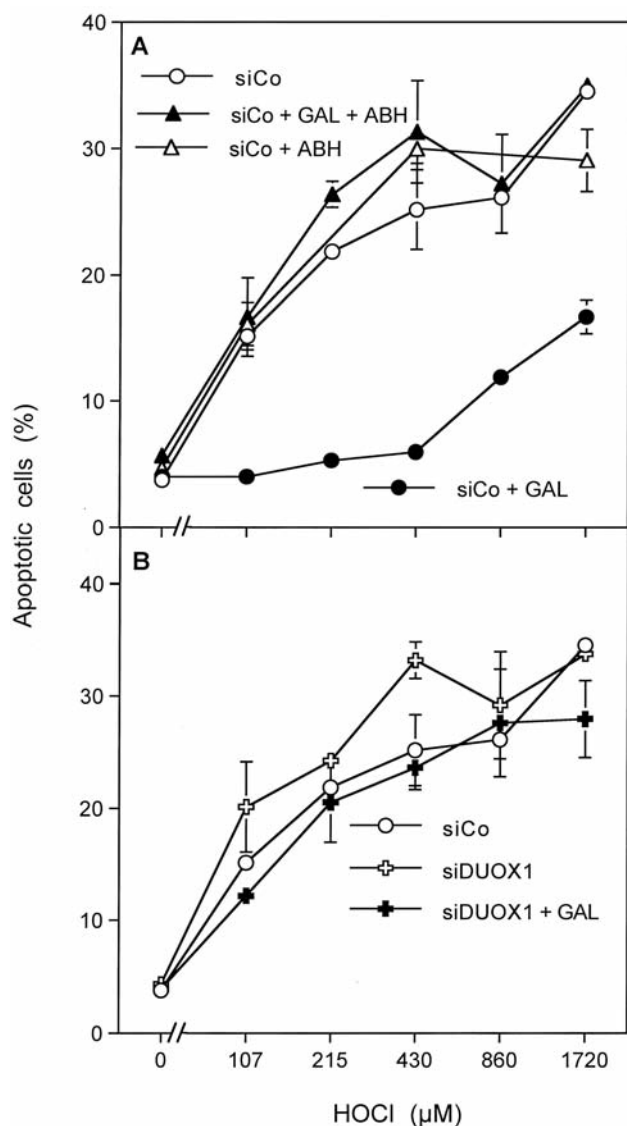


Figure 6. Membrane-associated dual oxidase 1 (DUOX1) protects against apoptosis induction by exogenous HOCl: reversal of the peroxidase reaction. Prevention of release of the DUOX1-coded peroxidase (POD) domain through application of galardin (GAL) renders MKN-45 cells resistant to the apoptosis-inducing effect of exogenous HOCl. Resistance is explained as catalytic decomposition of HOCl by POD, as it is prevented by the POD inhibitor 4-aminobenzoyl hydrazide (ABH). DUOX1 is defined as active POD, as small interfering RNA (siRNA)-mediated knockdown of DUOX1 (siDUOX1) abrogates the protective effect, whereas control siRNA (siCo) does not. Data are representative of five independent experiments.

now confined to the close vicinity of the cell membrane. This renders HOCl signaling non-responsive to inhibitory side-effects through superoxide anion/HOCl or ferrous ion/HOCl interactions distant from the membrane. These side-effects consume HOCl but generate hydroxyl radicals too far from the membrane to have a damaging effect on it.

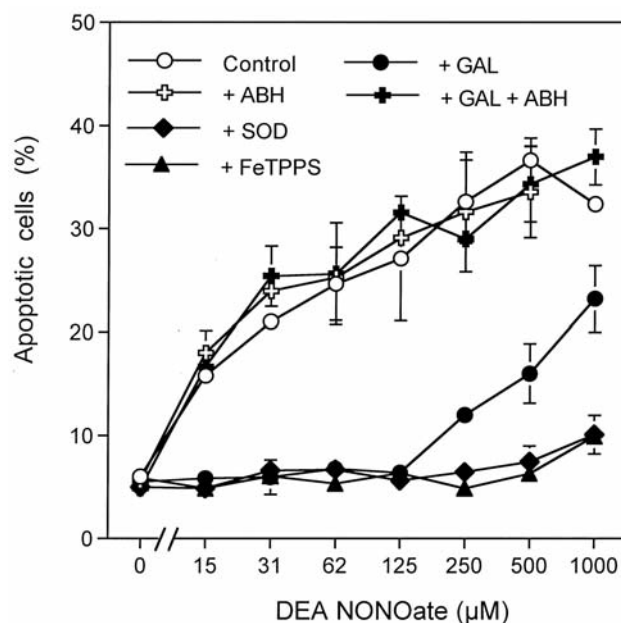
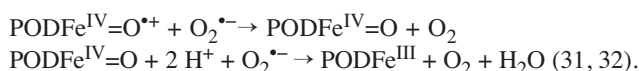


Figure 7. Membrane-associated dual oxidase 1 (DUOX1)-related peroxidase (POD) protects against apoptosis induction mediated by an exogenous NO donor. Prevention of release of the DUOX1-encoded peroxidase domain through application of galardin (GAL) renders 208Fsrc3 cells resistant to the apoptosis-inducing effect of the exogenous NO donor diethylamine (DEA NONOate). Resistance is prevented by the POD inhibitor 4-aminobenzoyl hydrazide (ABH). The apoptosis-inducing effect of the NO donor depends on the formation of peroxynitrite, as it is prevented by the superoxide anion scavenger superoxide dismutase (SOD) and the peroxynitrite decomposition catalyst 5-,10-,15-,20-tetrakis(4-sulfonatophenyl)porphyrinato iron(III) chloride (FeTPPS). Data are mean values  $\pm$  standard deviation. The presented experiment is representative of five independent experiments.

This optimizing effect of membrane-associated DUOX POD for HOCl signaling is contrasted by the potential of the localized enzyme to protect against exogenously added HOCl (Figure 12A). This protective effect was based on a catalytic reaction of POD, as it was inhibited by the POD inhibitor ABH. Based on these findings, the protective effect seems to be mediated by induction of the reverse reaction of POD, i.e. the decomposition of its reaction product HOCl. An analogous reverse reaction has been described for MPO (29, 30):



A catalytic cycle of HOCl destruction might be maintained by the interaction between  $\text{PODFe}^{\text{IV}}=\text{O}^{\bullet+}$  (compound I) and superoxide anions, involving  $\text{PODFe}^{\text{IV}}=\text{O}$  (compound II) as intermediate and resulting in  $\text{PODFe}^{\text{III}}$  (ferric POD), ready for the next cycle of HOCl destruction:



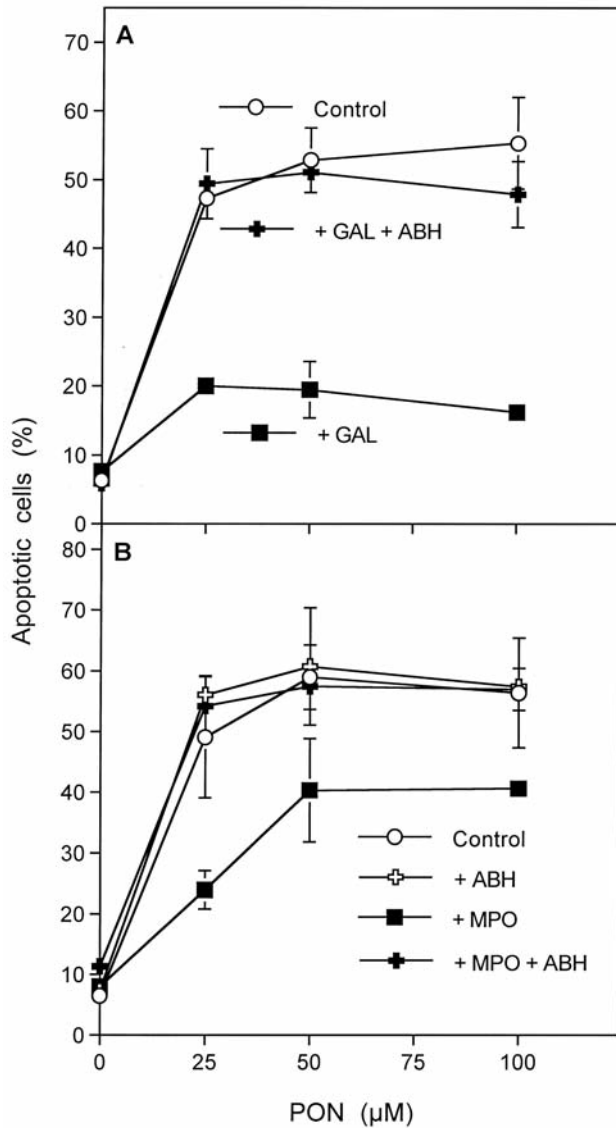


Figure 8. Membrane-associated DUOX1 peroxidase (POD) protects against apoptosis induction mediated by exogenous peroxynitrite. Prevention of release of the DUOX1-encoded POD domain through application of galardin (GAL) renders 208Fsrc3 cells resistant to the apoptosis-inducing effect of exogenous peroxynitrite (PON). Resistance is explained as catalytic decomposition of peroxynitrite by POD, as it is prevented by the POD inhibitor 4-aminobenzoyl hydrazide (ABH) (A). Addition of MPO has an analogous but weaker effect (B). Data are mean values  $\pm$  standard deviation. The presented experiment is representative of five independent experiments.

Membrane-associated DUOX1 has a strong protective effect against NO/peroxynitrite signaling (Figure 12B). In this respect, it acts analogously to membrane-associated catalase that interferes with NO/peroxynitrite signaling also through peroxynitrite decomposition and oxidation of NO. As membrane-associated DUOX1 protects against the apoptosis-

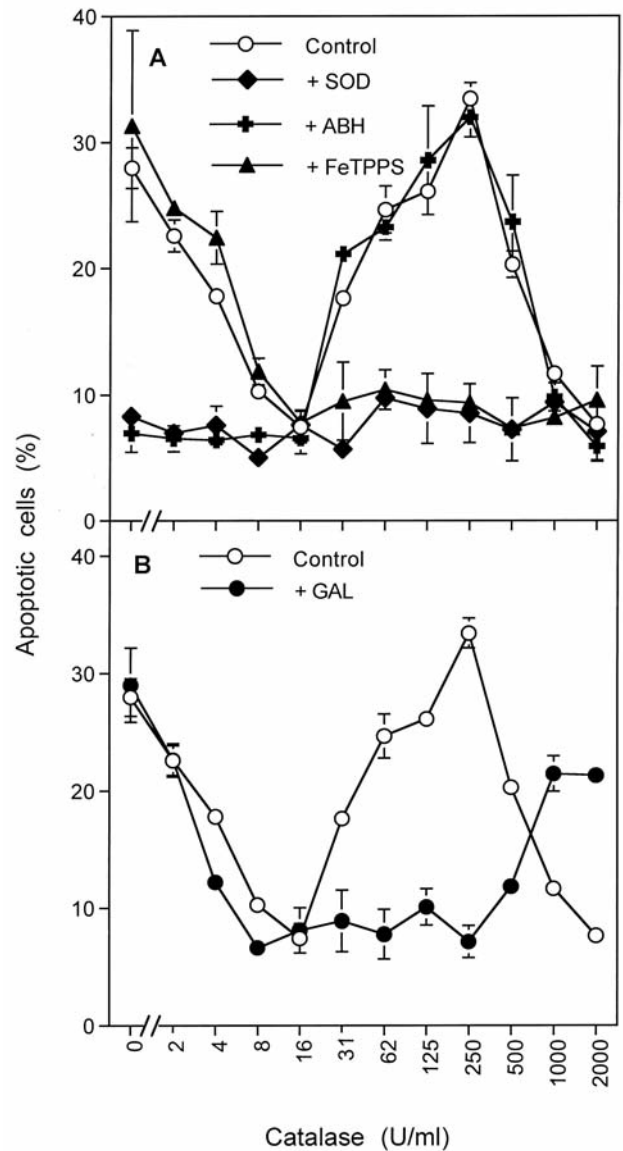


Figure 9. Selective inhibitory effect of galardin (GAL) on NO/peroxynitrite signaling of transformed cells. Autocrine apoptosis induction in transforming growth factor- $\beta$ 1 (TGF $\beta$ 1)-treated transformed 208Fsrc3 cells initially seems to depend on HOCl signaling, as it is inhibited by 4-aminobenzoyl hydrazide (ABH) and superoxide dismutase (SOD). With increasing concentration of added catalase, HOCl signaling is inhibited and signaling through the NO/peroxynitrite pathway (inhibition by 5-, 10-, 15-, 20-tetrakis(4-sulfonatophenyl)porphyrinato iron(III) chloride (FeTPPS) and SOD, but no inhibition by ABH) resumes but is inhibited at very high concentrations of soluble catalase (A). NO/peroxynitrite signaling is selectively inhibited by treatment with galardin (B). Data are mean values  $\pm$  standard deviation. The presented experiment is representative of two independent experiments.

inducing effect of exogenous peroxynitrite and as DUOX1 is related to MPO, it may be assumed that it utilizes the same or a similar mode of action for the destruction of

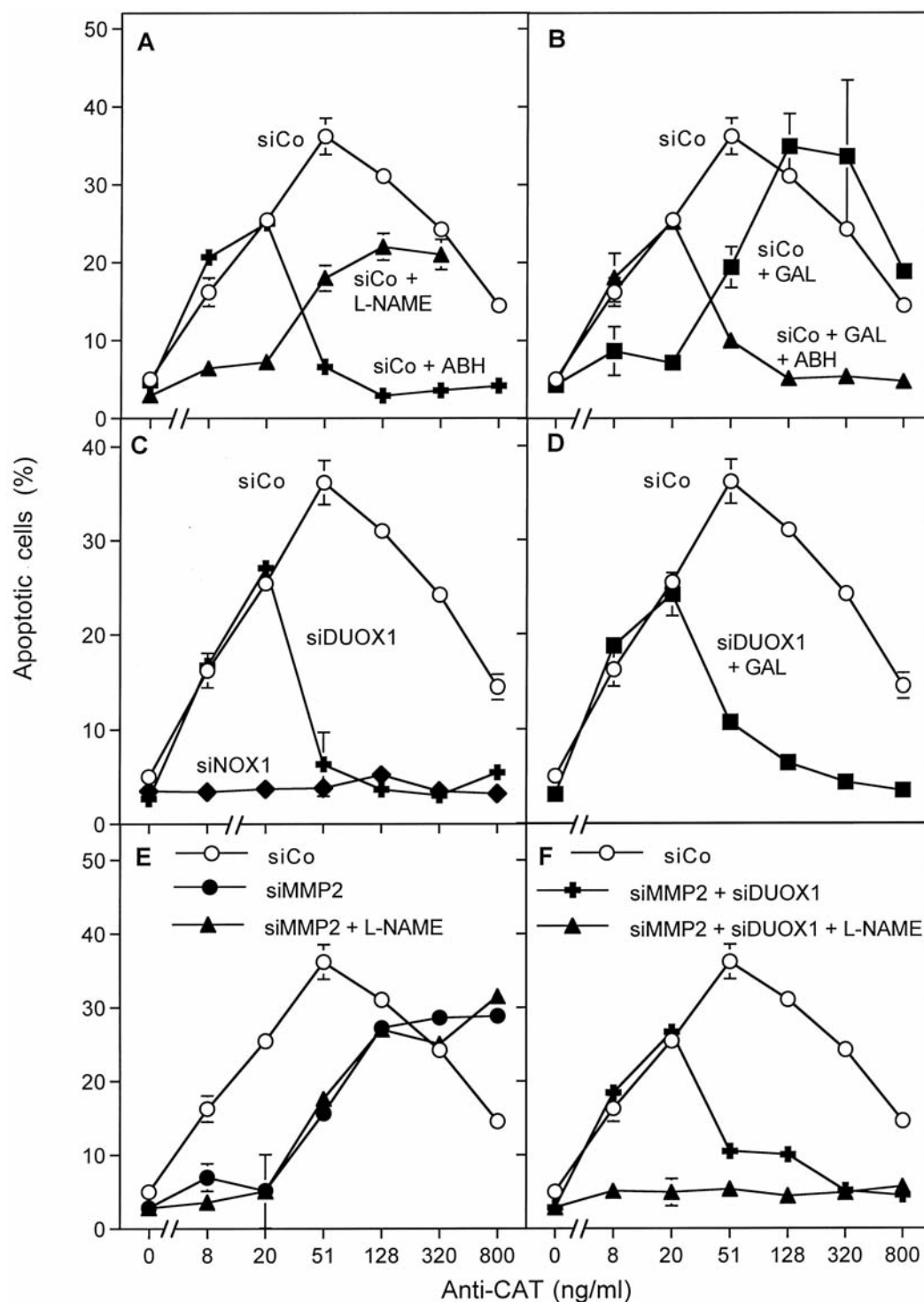


Figure 10. Selective inhibition of NO/peroxynitrite signaling in tumor cells with inactivated catalase through inhibition or knockdown of matrix metalloproteinase 2 (MMP2). The figure shows that autocrine apoptosis induction in MKN-45siCo cells (MKN-45 cells transfected with siCo for 24 h) in the presence of neutralizing antibodies directed towards catalase (anti-CAT) is mediated by the NO/peroxynitrite pathway at lower concentrations of anti-CAT, as it is inhibited by N-omega-nitro-L-arginine methylester hydrochloride (L-NAME), and the HOCl pathway at higher concentrations of anti-CAT, as it is inhibited by 4-aminobenzoyl hydrazide (ABH) (A). Galardin (GAL) treatment selectively inhibits NO/peroxynitrite signaling in MKN-45siCo cells (B). siRNA-mediated knockdown of dual oxidase 1 (DUOX1) selectively inhibits HOCl signaling and also prevents the galardin-mediated effect directed towards NO/peroxynitrite signaling (C and D). Knockdown of MMP2 causes an effect analogous to that of galardin treatment that is dependent on functional DUOX1 (E and F). Data are mean values  $\pm$  standard deviation. The presented experiment is representative of three independent experiments.



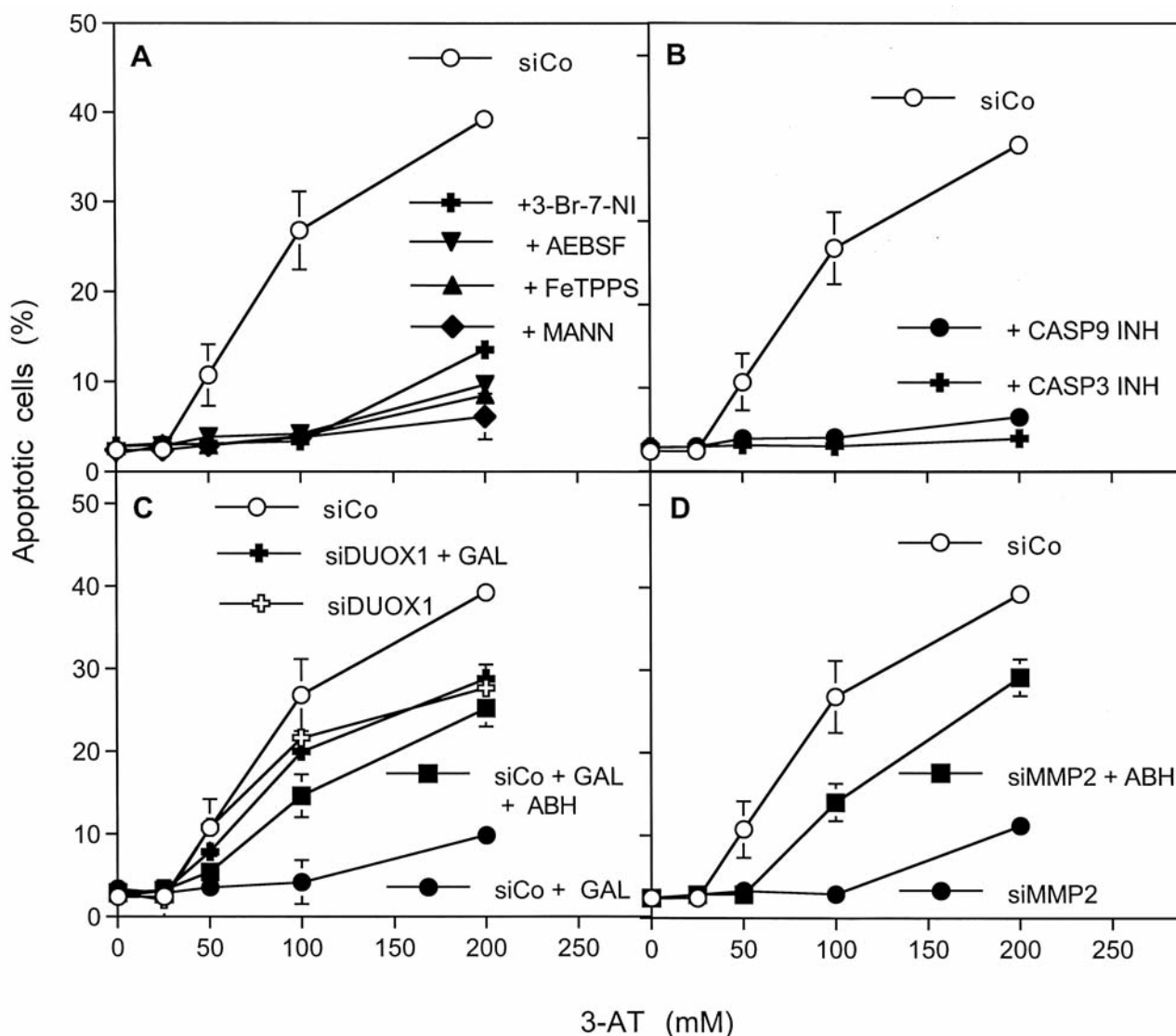
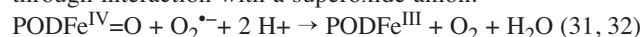


Figure 11. NO/peroxynitrite signaling in the Ewing sarcoma cell line SKN-MC is controlled by catalase and inhibited by galardin (GAL) treatment and knockdown of matrix metalloproteinase 2 (MMP2) using siMMP2. 3-aminotriazole (3-AT) causes autocrine apoptosis induction in SKN-MCsiCo cells that seems to be dependent on NO/peroxynitrite signaling, as it is inhibited by the NADPH oxidase 1 (NOX1) inhibitor 4-(2-aminoethyl)benzenesulfonyl fluoride (AEBSF), the NO synthase (NOS) inhibitor 3-bromo-7-nitroindazole (3-Br-7-NI), the peroxynitrite decomposition catalyst 5-,10-,15-,20-tetrakis(4-sulfonatophenyl)porphyrinato iron(III) chloride (FeTPPS) and the hydroxyl radical scavenger mannitol (MANN) (A). Autocrine apoptosis is mediated by caspase 3 and caspase 9, as it is inhibited by caspase 3 inhibitor (CASP3 INH) and caspase 9 inhibitor (CASP9 INH). (B). Galardin treatment interferes with autocrine apoptosis induction in siCo-transfected cells. Interference is abrogated by the peroxidase (POD) inhibitor 4-aminobenzoyl hydrazide (ABH) or siRNA-mediated knockdown of dual oxidase 1 (DUOX1) (C). Knockdown of MMP2 has an effect analogous to that of treatment with galardin (D). Data are mean values  $\pm$  standard deviation. The presented experiment is representative of three independent experiments.

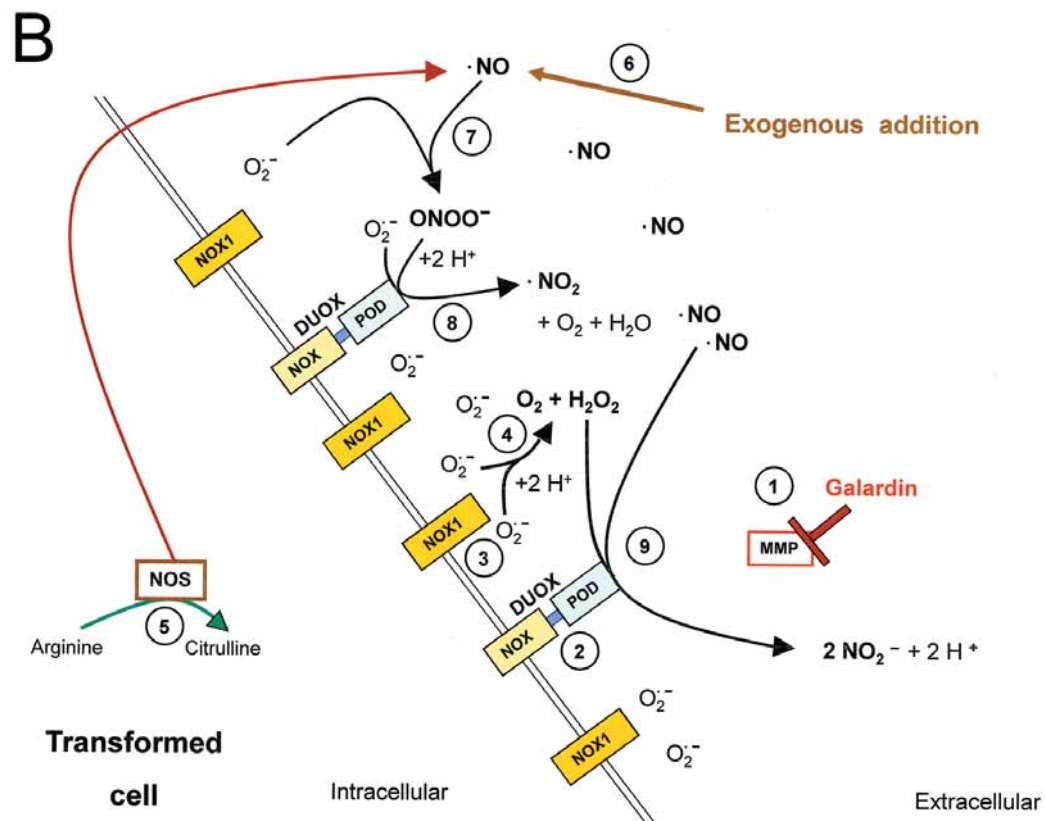
peroxynitrite as MPO. MPO has been shown to react with peroxynitrite (33-35), resulting in an intermediate composed of  $\text{PODFe}^{\text{IV}}=\text{O}^+$  and  $\text{NO}_2^-$  attached to the active center:  $\text{PODFe}^{\text{III}} + \text{ONOO}^- \rightarrow \text{PODFe}^{\text{IV}}=\text{O}^+ + \text{NO}_2^-$ . As a next step, internal reduction of  $\text{PODFe}^{\text{IV}}=\text{O}^+$  by  $\text{NO}_2^-$  leads to the generation of  $\text{PODFe}^{\text{IV}}=\text{O}$  and the release of  $\cdot\text{NO}_2$ :



$\text{PODFe}^{\text{IV}}=\text{O}$  may be brought back to the catalytic cycle through interaction with a superoxide anion:



In the presence of high concentrations of  $\text{H}_2\text{O}_2$ , an alternative reaction is conceivable that leads to the formation



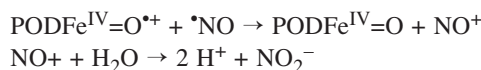
of the inactive  $\text{PODFe}^{\text{III}}\text{O}_2^{\bullet-}$  (compound III), *i.e.* a dead-end of POD activity:



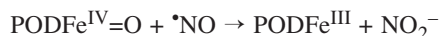
When the membrane-associated POD domain of DUOX was protective against peroxynitrite-mediated apoptosis induction after application of the NO donor DEA NONOate, it may not only have been acting on peroxynitrite generated through NO/superoxide anion interaction, but, in analogy to MPO, may also have oxidized NO and thus established a second line of defense against NO/peroxynitrite signaling. The localization at the membrane thereby established an optimal high local concentration of the protective POD domain, ensuring valuable kinetic advantages in the interaction with peroxynitrite, and possibly NO. The oxidation of NO by MPO (36), a mechanism that may also be applicable to DUOX1, first requires the formation of  $\text{PODFe}^{\text{IV}}=\text{O}^{\bullet+}$  (compound I) through the interaction between MPO and  $\text{H}_2\text{O}_2$ :

$\text{PODFe}^{\text{III}} + \text{H}_2\text{O}_2 \rightarrow \text{PODFe}^{\text{IV}}=\text{O}^{\bullet+} + \text{H}_2\text{O}$ .  
 $\text{PODFe}^{\text{IV}}=\text{O}^{\bullet+}$  then oxidizes one molecule of NO. The resultant nitrosium ion ( $\text{NO}^+$ ) readily reacts with water:

←



The interaction between  $\text{PODFe}^{\text{IV}}=\text{O}$  and NO then restores native POD:



Although the potential of membrane-associated DUOX POD to decompose peroxynitrite has been experimentally shown and the oxidation of NO by POD might be analogous to that of MPO, our data do not allow us to determine at which precise degree these two activities are involved in the protective effect against NO/peroxynitrite signaling. However, the partial abrogation of galardin-dependent inhibition of NO/peroxynitrite signaling at high concentrations of catalase (Figure 9) might be interpreted as consequence of impaired formation of  $\text{PODFe}^{\text{IV}}=\text{O}^{\bullet+}$  due to catalase activity and subsequent decrease of NO oxidation.

Finally, abrogation of galardin-dependent inhibition of NO/peroxynitrite signaling by DUOX at high concentrations of an exogenous NO donor (Figure 7) seems to indicate an inhibitory effect of NO on POD, in analogy to the interaction between NO and MPO (37). Our findings and published work of many other groups (14, 33-37) illustrate that heme-containing enzymes such as catalase and POD have more overlapping activities and more potential substrates than usually pointed-out in text books. The analogy in the interaction with NO and peroxynitrite between catalase and DUOX-related POD/MPO is especially striking, as both groups of enzymes i) are inhibited by NO; ii) can oxidize NO through a mechanism that involves the analogous active intermediates  $\text{PODFe}^{\text{IV}}=\text{O}^{\bullet+}$  or  $\text{CATFe}^{\text{IV}}=\text{O}^{\bullet+}$  and iii) can decompose peroxynitrite.

Our findings stress the significance of the localization of the enzymes studied. For example, the reverse reaction of DUOX-related POD, *i.e.* the decomposition of its reaction product, was only demonstrated when POD was attached to the membrane. In addition, protection against NO/peroxynitrite signaling required the localization of POD at the membrane, thus achieving a high local enzyme concentration at the site where peroxynitrite is generated through the interaction between NOX1-derived superoxide anions and cellular NO.

Our data show a dual mode of the action of DUOX-related POD. The enzyme is the central element for HOCl synthesis that establishes HOCl-dependent apoptosis signaling in transformed cells and tumor cells with inhibited membrane-associated catalase. This activity is independent to the localization of the POD. If attached to the membrane, DUOX-related POD protects transformed cells against NO/peroxynitrite signaling and establishes a second line of defense against NO/peroxynitrite signaling in tumor cells

Figure 12. Biochemical and cell biologically consequences of membrane association of dual oxidase (DUOX). A: Synthesis and destruction of HOCl. Inhibition of matrix metalloproteinases (MMP) by galardin (#1) prevents the release of the peroxidase domain (POD) of DUOX (#2). NADPH oxidase 1 (NOX1) (the hallmark of the transformed state) generates extracellular superoxide anions (#3) that form  $\text{H}_2\text{O}_2$  after dismutation (#4). Membrane-associated POD utilizes  $\text{H}_2\text{O}_2$  for the synthesis of HOCl (#5). HOCl/superoxide anion interaction (#6) leads to the formation of hydroxyl radicals that trigger apoptosis induction through lipid peroxidation (LPO) (#7). Confrontation of a transformed cell with membrane-associated POD by exogenous HOCl (e.g. from attacking neutrophils) (#8) leads to the induction of the reverse reaction of POD, *i.e.* decomposition of HOCl (#9) and protection of the transformed cell. In tumor cells that express membrane-associated catalase (not shown), reactions #5-7 would not take place as  $\text{H}_2\text{O}_2$  is decomposed by catalase. Reaction #9 would be effective in tumor cells and protect them against neutrophil-derived HOCl. B: Membrane-associated POD interferes with NO/peroxynitrite signaling. Inhibition of MMP (#1) prevents the release of the POD of DUOX (#2). NOX1 generates extracellular superoxide anions (#3) that form  $\text{H}_2\text{O}_2$  after dismutation (#4). NO is derived from cellular NO synthase (NOS) (#5) or from exogenous sources (e.g. cells of the innate immune system) (#6). The reaction between NO and superoxide anions leads to the formation of peroxynitrite (#7). Membrane-associated peroxidase decomposes peroxynitrite (#8) and thus prevents the formation of peroxynitrous acid and its homolysis into  $\text{NO}_2$  and apoptosis-inducing hydroxyl radicals (not shown). In addition, membrane-bound POD interferes with NO/peroxynitrite signaling through oxidation of NO (#9). Please see text for further details.

that have membrane-associated catalase as first line of defense. Even if catalase is inhibited or inactivated, the protection by membrane-associated DUOX-related POD seems to be protective. This is especially significant for the survival of tumor cell lines that establish primarily NO/peroxynitrite signaling. DUOX-related POD attached to the membrane also protects transformed and tumor cells against HOCl from exogenous sources through induction of the reverse reaction. It is conceivable that this function might be relevant for tumor cell escape from attack by HOCl-producing cells of the innate immune system. As the protective effects against NO/peroxynitrite signaling and against exogenous HOCl depend on the localization of the DUOX-related POD at the cell membrane and as MMPs counteract this localization, the activity of MMPs deserves specific attention for the understanding of the respective function of DUOX-related PODs.

## Acknowledgements

The Authors are grateful to Drs. C. Sers and R. Schäfer (Berlin) for the gift of 208F and 20Fsrc3 cells and to Dr. U. Kontny (Freiburg) for SKN-MC cells. We thank the COST consortium "ChemBioRadical" (COST Action CM0603) organized by C. Chatgililoglu (Bologna) for intellectual support and constructive criticism. This study was funded by EuroTransBio.

## References

- Irani K, Xia Y, Zweier JL, Sollott SJ, Der CJ, Fearon ER, Sundaresan M, Finkel T and Goldschmidt-Clermont PJ: Mitogenic signalling by oxidants in Ras-transformed fibroblasts. *Science* 275: 1649-1652, 1997.
- Suh Y-A, Arnold RS, Lassegue B, Shi J, Xu X, Sorescu D, Chung AB, Griendling KK and Lambeth JD: Cell transformation by the superoxide-generating oxidase Mox1. *Nature* 401: 79-82, 1999.
- Yang JQ, Li S, Domann FE, Buettner G and Oberley LW: Superoxide generation in v-Ha-ras-transduced human keratinocyte HaCaT cells. *Mol Carcinogenesis* 26: 180-188, 1999.
- Arnold RS, Shi J, Murad E, Whalen AM, Sun CQ, Palavarapu R, Parthasarathy S, Petros JA and Lambeth JD: Hydrogen peroxide mediates the cell growth and transformation caused by the mitogenic oxidase Nox1. *Proc Natl Acad Sci USA* 98: 5550-5555, 2001.
- Schwieger A, Bauer L, Hanusch J, Sers C, Schäfer R and Bauer G: Ras oncogene expression determines sensitivity for intercellular induction of apoptosis. *Carcinogenesis* 22: 1385-1392, 2001.
- Mitsushita J, Lambeth JD and Kamata T: The superoxide-generating oxidase Nox1 is functionally required for Ras oncogenic transformation. *Cancer Res* 64: 3580-3585, 2004.
- Herdener M, Heigold S, Saran M and Bauer G: Target cell-derived superoxide anions cause efficiency and selectivity of intercellular induction of apoptosis. *Free Rad Biol Med* 29: 1260-1271, 2000.
- Heigold S, Sers C, Bechtel W, Ivanovas B, Schäfer R and Bauer G: Nitric oxide mediates apoptosis induction selectively in transformed fibroblasts compared to nontransformed fibroblasts. *Carcinogenesis* 23: 929-941, 2002.
- Bauer G: Tumor cell protective catalase as a novel target for rational therapeutic approaches based on specific intercellular ROS signaling. *Anticancer Res* 32: 2599-2624, 2012.
- Bauer G: Targeting extracellular ROS signaling of tumor cells. *Anticancer Res* 34: 1467-1482, 2014.
- Kundráť P, Bauer G, Jacob P and Friedland W: Mechanistic modelling suggests that the size of preneoplastic lesions is limited by intercellular induction of apoptosis in oncogenically transformed cells. *Carcinogenesis* 33: 253-259, 2012.
- Bauer G: Increasing the endogenous NO level causes catalase inactivation and reactivation of intercellular apoptosis signaling specifically in tumor cells. *Redox Biol*, 6: 353-371, 2015.
- Bechtel W and Bauer G: Catalase protects tumor cells against apoptosis induction by intercellular ROS signaling. *Anticancer Res* 29: 4541-4557, 2009.
- Heinzelmann S and Bauer G: Multiple protective functions of catalase against intercellular apoptosis-inducing ROS signaling of human tumor cells. *Biol Chem* 391: 675-693, 2010.
- Santiskulvong C and Rozengurt E: Galardin (GM 6001), a broad-spectrum matrix metalloproteinase inhibitor, blocks bombesin- and LPA-induced EGF receptor transactivation and DNA synthesis in Rat-1 cells. *Exp Cell Res* 290: 437-446, 2003.
- Bauer G, Höfler P and Simon M: Epstein-Barr virus induction by a serum factor II. Purification of a high molecular weight protein that is responsible for induction. *J Biol Chem* 257: 11405-11410, 1982.
- Quade K: Transformation of mammalian cells by avian myelocytomatosis virus and avian erythroblastosis virus. *Virology* 98: 461-465.
- Iten E, Ziemecki A and Schäfer R: The transformation-suppressive function is lost in tumorigenic cells and is restored upon transfer a suppressor gene. *Recent Results Cancer Res* 113: 78-89, 1989.
- Temme J and Bauer G: Low-dose gamma irradiation enhances superoxide anion production by nonirradiated cells through TGF- $\beta$ 1-dependent bystander signaling. *Rad Res* 179: 422-432, 2013.
- Bauer G: Low dose irradiation enhances specific signaling components of intercellular reactive oxygen-mediated apoptosis induction. *J Phys Conf ser* 261 012001, 2011.
- Wyllie AH, Kerr JF and Currie AR: Cell death: the significance of apoptosis. *Int Rev Cytol* 68: 251-274, 1980.
- Elmore S: Apoptosis: a review of programmed cell death. *Toxicol Pathol* 35: 495-516, 2007.
- Jürgensmeier J, Schmitt CP, Viesel E, Höfler P and Bauer G: TGF $\beta$ -treated normal fibroblasts eliminate transformed fibroblasts by induction of apoptosis. *Cancer Res* 54: 393-398, 1994.
- Beck E, Schäfer R and Bauer G: Sensitivity of transformed fibroblasts for intercellular induction of apoptosis is determined by their transformed phenotype. *Exp Cell Res* 234: 47-56, 1997.
- Bauer G, Bereswill S, Aichele P and Glocker E: Helicobacter pylori protects protects oncogenically transformed cells from reactive oxygen species-mediated intercellular induction of apoptosis. *Carcinogenesis* 35: 1582-1591, 2014.



- 26 Bauer G and Zarkovic N: Revealing mechanisms of selective, concentration-dependent potentials of 4-hydroxy-2-nonenal to induce apoptosis in cancer cells through inactivation of membrane-associated catalase. *Free Rad Biol Med* 81: 128-144, 2015.
- 27 Bauer G, Chatgililoglu C, Gebicki JL, Gebicka L, Gescheidt G, Golding BT, Goldstein S, Kaizer J, Merenyi G, Speier G and Wardman P: Biologically relevant small radicals. *Chimia* 62: 1-9, 2008.
- 28 Bauer G: HOCl-dependent singlet oxygen and hydroxyl radical generation modulate and induce apoptosis of malignant cells. *Anticancer Res* 33: 3589-3602, 2013.
- 29 Floris R and Wever R: Reaction of myeloperoxidase with its product HOCl. *Eur J Biochem* 207: 697-702, 1992.
- 30 Furtmüller PG, Burner U, Jantschko W, Regelsberger G and Obinger C: The reactivity of myeloperoxidase compound I formed with hypochlorous acid. *Redox Rep* 5: 173-178, 2000.
- 31 Kettle AJ and Winterbourn CC: Superoxide modulates the activity of myeloperoxidase and optimizes the production of hypochlorous acid. *Biochem J* 252: 529-536, 1988.
- 32 Winterbourn CC, Hampton MB, Livesey JH and Kettle AJ: Modeling the reactions of superoxide and myeloperoxidase in the neutrophil phagosome. *J Biol Chem* 281: 39860-3986, 2006.
- 33 Floris R, Piersma SR, Yang G, Jones P and Wever R: Interaction of myeloperoxidase with peroxynitrite. A comparison with lactoperoxidase, horseradish peroxidase and catalase. *Eur J Biochem* 215: 767-775, 1993.
- 34 Gebicka L and Gebicki JL: Reactions of heme peroxidases with peroxynitrite. *IUBMB Life* 49: 11-15, 2000.
- 35 Furtmüller PG, Jantschko W, Zederbauer M, Schwanninger M, Jakopitsch C, Herold S, Koppenol WH and Obinger C: Peroxynitrite efficiently mediates the interconversion of redox intermediates of myeloperoxidase. *Biochem Biophys Res Comm* 337: 944-954, 2005.
- 36 Abu-Soud HM and Hazen SL: Nitric oxide is a physiological substrate for mammalian peroxidases. *J Biol Chem* 275: 37524-37532, 2000.
- 37 Abu-Soud HM and Hazen SL: Nitric oxide modulates the catalytic activity of myeloperoxidase. *J Biol Chem* 275: 5425-5430, 2000.

*Received June 23, 2015*  
*Revised September 5, 2015*  
*Accepted September 9, 2015*